Journal of Catalysis **194,** 45–54 (2000)
doi:10.1006/jcat.2000.2909, available online at http://www.idealibrary.com on IDEAL®

Study of Adsorption and Reactions of Methyl Iodide on TiO_2

C. Su,*[,1] J.-C. Yeh,† C.-C. Chen,† J.-C. Lin,*[,2] and J.-L. Lin†[,2]

*Institute of Atomic and Molecular Sciences, Academia Sinica, P.O. Box 23-166, Taipei, 106, Taiwan; and †Department of Chemistry, National Cheng Kung University, Tainan, 701, Taiwan

Received October 19, 1999; revised March 17, 2000; accepted May 1, 2000

The adsorption, thermal reactions, and photochemistry of methyl iodide were studied on powdered TiO_2 by transmission infrared spectroscopy, and on a TiO_2(110) single-crystal surface by temperature-programmed desorption (TPD) and X-ray photoemission spectroscopy (XPS). CH_3I is either adsorbed molecularly or adsorbed dissociatively, forming methoxy groups on powdered TiO_2 by thermal activation as observed by IR spectroscopy. The dissociation of CH_3I is enhanced by the presence of surface hydroxyl groups. $CH_{4(g)}$ evolves thermally as a major product when CH_3I reacts with powdered TiO_2 in the absence of oxygen. However, only oxygen-containing reaction intermediates and products are found when oxygen is present, including $CH_2O_{(g)}$, $(CH_3)_2O_{(g)}$, $CO_{(g)}$, $CO_{2(g)}$, and $H_2O_{(g)}$. $(CH_3)_2O_{(g)}$ is formed via a coupling reaction of two adsorbed methoxy groups. For the thermal reactions on TiO_2(110), desorption of $(CH_3)_2O_{(g)}$ is observed at multilayer coverages by TPD study. The formation of $(CH_3)_2O_{(g)}$ on TiO_2(110) occurs at much lower temperatures. It starts to evolve at ~200 K and reaches its maximum rate at 250–330 K depending on surface heterogeneity in the TPD study. The Williamson synthesis process is proposed for the generation of $(CH_3)_2O_{(g)}$ in this case. In addition, surface iodine formed by X-ray irradiation on CH_3I-covered TiO_2 is not stable and is desorbed by 570 K. In the photochemistry of CH_3I over powdered TiO_2, when O_2 is absent, negligible reactions occur. In the presence of O_2, some CH_3I is photooxidized to surface formate groups and $CO_{2(g)}$. This reaction is most likely initiated by superoxide, O_2^-, formed upon irradiation.

Key Words: **methyl iodide; TiO_2; thermal reaction; photochemistry; powder; single crystal; FT-IR; XPS; TPD.**

INTRODUCTION

The adsorption and dissociation of alkyl halides on metals (1), oxygen-preadsorbed metals (2–4), and oxide-supported metal catalysts (5–8) have been the subject of intense studies. This is because alkyl halides are useful precursors to generate alkyl groups adsorbed on various metal surfaces. Alkyl groups bound to metal surfaces are postulated as important surface intermediates in many catalytic processes, such as Fischer–Tropsch synthesis, oxidative dimerization of methane, and chemical vapor deposition using organometallic compounds (1). Recently, there is great interest in the chemistry of alkyl halides on oxide-supported metal catalysts, attempting to delineate the reaction affecting factors on these composite systems (5–8). In addition to the catalysis aspect, destruction of hazardous halogenated organic compounds using metal oxide surfaces has been the focal point in the research on environmental protection (9, 10).

Previously, Wong *et al.* studied the adsorption and photooxidation of CH_3Cl on a TiO_2(110) single crystal and on powdered TiO_2(11). It is found that CH_3Cl is adsorbed molecularly on TiO_2(110) and is desorbed from the surface by 230 K. CH_3Cl also remains intact on powdered TiO_2 at 315 K. Here, we investigate the adsorption, thermal reactions, and photochemistry of CH_3I on powdered TiO_2. The C–I bond energy is ~30 kcal/mol lower than that of the C–Cl bond. It is intriguing to explore the possibility of breaking the C–I bond and follow the reaction pathways of the CH_3 group and iodine. Furthermore, because there are residual hydroxyl groups on the surface after our TiO_2 sample treatment, the effect of its presence on CH_3I dissociation is also studied. Recently, Garrett *et al.* have studied the adsorption and photochemistry on TiO_2(110) (12, 13). In the present work, the reaction of CH_3I on TiO_2(110) is studied for higher coverages that were not covered in Garrett's paper and the results are compared to those obtained for powdered TiO_2. In addition, the photochemistry of CH_3I over powdered TiO_2 in the absence and in the presence of oxygen is investigated as well.

EXPERIMENTAL

The experiments were carried out in two separate vacuum systems to employ different techniques to study the reactions of CH_3I on powdered TiO_2 and on single-crystal TiO_2 surfaces, respectively. The system used for the powdered TiO_2 study and its IR cell have been described

[1] Present address: Institute of Organic and Polymeric Materials, National Taipei University of Technology, Taipei, 106, Taiwan, R.O.C.

[2] To whom correspondence should be addressed. J.-C.L.: Fax: 886-2-23620200; E-mail: jclin@po.iams.sinica.edu.tw. J.-L.L.: Fax: 886-6-2740552; E-mail: jonglin@mail.ncku.edu.tw.

0021-9517/00 $35.00

previously (14). Briefly, the IR cell equipped with two CaF_2 windows for IR transmission was connected to a gas manifold pumped by a 60 l s^{-1} turbomolecular pump to reach a base pressure of $\sim 1 \times 10^{-7}$ Torr. The pressure of the system was measured with a Baratron capacitance manometer and an ion gauge. The powdered TiO_2 used in the study was supported on a tungsten grid of ~ 6 cm^2. This grid was held in a pair of stainless steel clamps which were attached to the power leads of a power/thermocouple feedthrough. The sample temperature was measured by a K-type thermocouple spot-welded on the top of the W-grid. Samples were made by spraying onto the W-grid a slurry of TiO_2 powder (Degussa P25, ~ 50 m^2/g, anatase $\sim 70\%$ and rutile $\sim 30\%$) dispersed in a mixture of water and acetone. The TiO_2 sample was then mounted into the IR cell for *in situ* monitoring of the reaction process by Fourier transform infrared spectroscopy (FTIR) and thoroughly outgassed at 723 K for 24 h under vacuum. Before each run of the experiment, the TiO_2 sample was heated to 723 K for 2 h. When the sample was cooled to 343 K after the heating, 10 Torr of O_2 was introduced into the cell while the sample's temperature decreased continuously. As the temperature reached 308 K, the cell was evacuated for gas dosing. This procedure caused surface dehydration and removed adsorbed hydrocarbons, but a small amount of residual hydroxyl groups still existed (15). This surface was also highly defective, resulting from inherent poorly organized surface atoms on powder particles and from the surface annealing process in vacuum. For prolonged annealing at 723 K in vacuum, the TiO_2 powder sometimes turned a light gray color.

In the photoreaction study, both the IR beam and the irradiation light for inducing photochemistry were 45° to the normal of W-grid. The UV light source for the photochemistry study was constituted by an Hg arc lamp (350 W, Oriel Corp.), a water filter, and a band-pass filter (Oriel 51670) with ~ 100 nm bandwidth centered at ~ 400 nm. The power at the position of the TiO_2 sample was ~ 0.14 W/cm^2 measured in the air by a power meter (Molectron, PM10V1). Infrared spectra were obtained with 4 cm^{-1} resolution by a Bruker Fourier transform infrared spectrometer with an MCT detector. The entire optical path was purged with CO_2-free dry air. Each spectrum presented in this paper has been ratioed against clean TiO_2 spectra.

The reactions of CH_3I on the $TiO_2(110)$ surface were investigated in a two-level ultrahigh vacuum (UHV) system with a routine base pressure below 5×10^{-10} Torr. A detailed description of the system design has been given previously (16). Briefly, the chamber was equipped with a four-grid reverse viewing low-energy electron diffraction (LEED) optics (VG, RVL-900) for surface structure determination, an Auger electron spectrometer (AES) for surface elemental analysis, an ion sputtering gun (PHI 04-177) for $TiO_2(110)$ surface cleaning, and a quadrupole mass spectrometer (QMS) (UTI, 0-300 amu) for temperature-programmed desorption experiments. The QMS was situated in a copper tube and separated from the main chamber by an Mo cone with a 2-mm-diameter aperture, and differentially pumped with two small ion pumps (20 L s^{-1}).

The $TiO_2(110)$ single crystal (10 mm × 10 mm × 1 mm) used in this study was obtained from Commercial Crystal Laboratories Inc. The crystal was first treated by ultrasonic cleaning in acetone and methanol solvents to remove organic contaminants on the surface and then was fastened to a 1-mm-thick tantalum (Ta) supporting plate with a gold foil placed in between for intimate thermal contact (17). Two Ta wires (0.5 mm diameter) were spot-welded on the back side of the Ta supporting plate and connected to the power feedthrough. Variation of the temperature of the TiO_2 sample assembly was achieved by a combination of liquid-nitrogen cooling and resistive heating via the Ta wires.

The $TiO_2(110)$ surface temperature was monitored by a K-type thermocouple spot-welded onto a tiny bend-over Ta tab which was inserted into a precut slot at one of the corners of the crystal as shown in Fig. 1. Computer software was employed to linearly control the TiO_2 temperature between 100 and 1000 K and to record multiple QMS signals simultaneously for TPD study.

The TiO_2 crystal was cleaned by Ar^+ ion bombardment (500 eV, 10 min, current ~ 2 μA). Surface cleanliness was frequently checked by AES. The surface stoichiometry was achieved by annealing the cleaned surface at 1000 K for 3 min in 2×10^{-6} Torr of O_2 followed by cooling to room temperature (10 min) at the same oxygen pressure. The crystal color changed from transparent to dark blue after heating of the crystal to 1000 K under vacuum. This surface is also called a "smoothed surface" hereafter in the following TPD study. After the treatment, a (1×1) LEED pattern with sharp diffraction spots was obtained. XPS showed sharp Ti 2*p* peaks with no obvious indication of a reduced Ti state. There were fully coordinated and five-fold-coordinated Ti^{+4} cations present on this surface.

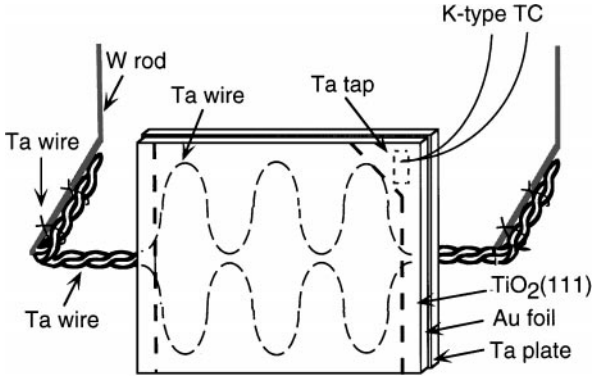

FIG. 1. Schematic showing the design of the sample holder for the $TiO_2(110)$ single crystal.

However, there might also exist, even in a small amount, surface defect sites, such as lattice oxygen vacancy, single bridging oxygen vacancy, and double bridging oxygen vacancy (18). Note that there were no surface hydroxyl groups on this single-crystal surface after the cleaning and annealing treatment. The previous study by Pan *et al.* (19) has shown that annealing TiO_2 in a vacuum or sputtering the surface causes a slightly oxygen-deficient or highly oxygen-deficient TiO_2(110) surface, respectively. Due to the loss of the surface oxygen atoms, there are several Ti reduced states present on the surface as observed by XPS (19). The sputtered surface also loses the long-range order as suggested by the appearance of vague LEED image.

Methyl iodide (99.5%, Aldrich), shielded from light, was purified by several cycles of freeze–pump–thaw before introduction into the IR cell or the UHV chamber. The O_2 gas used was purchased from Matheson with 99.998% purity.

RESULTS

Adsorption of CH_3I and Formation of CH_3O on Powdered TiO_2

Figure 2a shows the infrared spectrum of TiO_2 at 308 K in contact with 2 Torr of CH_3I. Below 3100 cm^{-1}, absorption bands appear at 1245, 1261, 2832, 2927, 2955, 2980, and 3050 cm^{-1}. Above 3100 cm^{-1}, a broad band centered at ~3535 cm^{-1} and negative bands in the region of 3600–3750 cm^{-1} are observed. Since CH_3I is present in the gas phase of the reaction system, it is expected that its absorption bands appear in Fig. 2a. To locate their positions, a CH_3I gaseous infrared spectrum (Fig. 2b) was obtained in a separate experiment using the same optical operating condition as those for Fig. 2a. Four major bands at 1240, 1261, 2959, and 2980 cm^{-1} are observed. By comparing the band frequencies and their relative intensities for Figs. 2a and 2b, it is concluded that the bands of 1245, 2832, 2927, 2955, and 3050 cm^{-1} in Figure 2a are not due to CH_3I in the gas phase. In the previous study of TiO_2 at 315 K in contact with CH_3Cl, Wong *et al.* observed that the adsorbed CH_3Cl exhibits infrared absorptions at 1236, 1444, and 2964 cm^{-1} (11). Based on Wong's result, the bands at 1245, 2955, and 3050 cm^{-1} in Fig. 2a are thus attributed to CH_3I absorbed on the TiO_2. These absorption frequencies are assigned to CH_3 symmetric deformation, symmetric stretch, and antisymmetric stretch, respectively (20). When the reaction system of TiO_2 in 2 Torr of CH_3I was evacuated, it is found that absorption bands due CH_3I either in the gas phase or on the surface disappear. It is worth noting that the bands of 1245, 2955, and 3050 cm^{-1} are not due to CH_3I in a multilayer, but instead due to CH_3I directly bonded to the TiO_2 surface. This conclusion is based on two reasons. In the previous TiO_2(110) TPD study, Garrett *et al.* observed that CH_3I is desorbed from multilayer by 220 K (12, 13). In addition, in terms of the relationship of temperature–pressure for the CH_3I vapor–liquid equilibrium system (21), the temperature needed to condense 2 Torr of CH_3I into a multilayer liquid phase is much lower than 308 K. Furthermore, although the band at 2832 cm^{-1} may also be assigned to the overtone of CH_3 antisymmetric deformation (20), the simultaneous presence of 2832 and 2927 cm^{-1} indicates the formation of methoxy groups on TiO_2. The identification of adsorbed methoxy groups ($CH_3O_{(a)}$) from dissociative CH_3OH adsorption on TiO_2 by infrared spectroscopy has been reported previously (22–25). The negative bands at 3600–3750 cm^{-1} show the decrease of surface hydroxyl groups on TiO_2 after the adsorption of CH_3I. This reduction may be partly due to H-bonding interaction of the hydroxyl groups with the adsorbed CH_3I, as supported by the appearance of the broad feature centered at ~3535 cm^{-1}. Figure 2c shows the spectrum taken at 343 K after the TiO_2 initially in 2 Torr of CH_3I at 308 K was heated to 343 K and maintained at this temperature for 90 min. Several changes of adsorption features occur due to this TiO_2 annealing treatment. First, the peaks due to methoxy groups grow with the surface annealing and shift slightly to higher frequencies of 2835 and 2935 cm^{-1}. Second, the diminishing band intensities of adsorbed CH_3I indicate that its adsorbed amount decreases with increasing surface temperature and this is in part due to the possible site-blocking effect of adsorbed methoxy groups and in part due to thermal desorption. Third, because of the changes

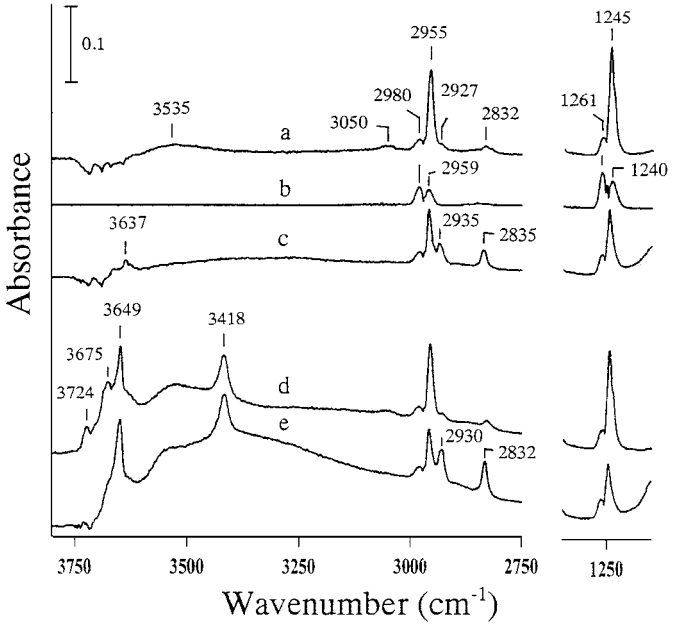

FIG. 2. (a) IR spectrum of the TiO_2 at 308 K in contact with 2 Torr of CH_3I. (b) IR spectrum of 4 Torr of CH_3I. (c) IR spectrum recorded at 343 K after the TiO_2 initially in 2 Torr of CH_3I at 308 K was heated to 343 K and held at this temperature for 90 min. (d) IR spectrum of the hydroxylated TiO_2 at 308 K in contact with 2 Torr of CH_3I. (e) IR spectrum taken at 343 K after the hydroxylated TiO_2 initially in 2 Torr of CH_3I was heated to 343 K and maintained at this temperature for 90 min. All of the spectra were taken with 50 scans. The TiO_2 sample used was ~68 mg.

in surface adsorption as mentioned above, the absorption features in the hydroxyl stretching region are also affected. The broad feature at ~3535 cm^{-1} almost disappears, accompanied with a new absorption at 3637 cm^{-1}. This reflects the changes in the hydroxyl local bonding environment. Since in our TiO_2 sample preparation process, surface hydroxyl groups cannot be completely removed, the effect of the surface hydroxyl groups on the CH_3I adsorption and reaction on TiO_2 was therefore further studied. To prepare a hydroxylated TiO_2 surface, a clean TiO_2 surface was exposed to 1 Torr of H_2O vapor at 308 K, followed by annealing at 423 K for 1 min and evacuating at 443 K for 5 min to remove adsorbed water (26). Figure 2d shows the infrared spectrum for the hydroxylated TiO_2 in contact with 2 Torr of CH_3I at 308 K. Below 3100 cm^{-1}, the infrared absorption features are similar to those in Fig. 2a, except that the intensities of 1245 and 2955 cm^{-1} from adsorbed CH_3I are ~10% less. Above 3000 cm^{-1}, four bands, situated on a broad adsorption feature extended from ~3000 to 3750 cm^{-1}, appear at 3418, 3649, 3675, and 3724 cm^{-1}. Previously, IR band assignments for TiO_2 surface hydroxyl groups have been reported in the literature (26–31). Primet *et al.* have found that surface hydroxyl groups absorb at 3410, 3655, and 3685 cm^{-1} on rutile TiO_2 as well as at 3665 and 3715 cm^{-1} on anatase TiO_2. The 3685 and 3715 cm^{-1} bands are assumed to be isolated hydroxyls and the others are reasoned to result from hydroxyl groups bonded to each other by hydrogen bridges (27). However, Tanaka and White have assigned the bands at 3676 and 3715 cm^{-1} on anatase TiO_2 to isolated hydroxyls bonded to Ti ions with different coordination or on different anatase faces (26). In terms of the Tanaka assumption, the lower amount of adsorbed CH_3I on hydroxylated TiO_2 as observed in Fig. 2d is probably related to the hydroxyl site-blocking effect. Very likely, CH_3I is interacting via the lone pair electrons on the iodine atom with the Ti ions on TiO_2. Therefore, the amount of CH_3I adsorption is reduced by the presence of hydroxyl groups occupying the Ti ion sites. Figure 2e shows the spectrum taken at 343 K after the hydroxylated TiO_2 initially in 2 Torr of CH_3I at 308 K was heated to 343 K and kept at this temperature for 90 min. The bands at 2832 and 2930 cm^{-1} from methoxy groups increase in intensity with the surface annealing treatment at 343 K. However, due to the surface hydroxylation, its amount is twice that in Fig. 2c. Meanwhile, the isolated hydroxyl peaks at 3675 and 3724 cm^{-1} disappear, whereas the 3418 and 3649 cm^{-1} peaks of the hydroxyl groups involving in hydrogen bonding remain unchanged. This indicates that the latter types of hydroxyl groups lack reactivity toward CH_3I.

Thermal Reactions of CH_3I on Powdered TiO_2

Figure 3 shows the infrared spectra taken at the indicated temperatures during linear heating of the TiO_2 sample at a rate of 2 K/s (from 308 to 673 K) in the presence of ~20 Torr of CH_3I. The spectrum recorded at 433 K resembles the one for gaseous CH_3I. The absorptions due to adsorbed CH_3I are not obvious in this spectrum, because a lower amount of TiO_2 was used in this experiment and its absorptions may be buried in the large absorption bands of CH_3I in the gas phase. Following thermal activation, peaks appears at 1307 (not shown) and 3017 cm^{-1}, revealing the formation of methane in the gas phase (32). Methane starts to evolve at ~623 K and is the major product detected. A small amount of CO_2 is also observed at 2349 cm^{-1}. When oxygen is present in the reaction system, the reaction pathways are completely different. Figure 4 shows the infrared spectra recorded at the indicated temperatures during heating of the TiO_2 at a rate of 2 K/s up to 673 K in the presence of a mixture of ~25 Torr of CH_3I and ~70 Torr of O_2. No methane is detected in the reaction system throughout the heating process. Instead, only partially oxidized intermediates and fully oxidized products are observed, including dimethyl ether ($(CH_3)_2O_{(g)}$, 1178 cm^{-1}), formaldehyde ($CH_2O_{(g)}$, 1745 cm^{-1}), carbon monoxide ($CO_{(g)}$, 2143 cm^{-1}), carbon dioxide ($CO_{2(g)}$, 2349 cm^{-1}), and water ($H_2O_{(g)}$, 1653 cm^{-1}) (32). The relative concentrations of water, carbon monoxide, carbon dioxide, formaldehyde, dimethyl ether, and unreacted methyl iodide as a function of TiO_2 temperatures are plotted in Fig. 5a. Formation of the oxygen-containing compounds and their temperature-dependent behavior are similar to those of methanol interacting with TiO_2. In the methanol case, previous studies have shown that these compounds are due to the reaction of adsorbed methoxy groups with TiO_2 surfaces (23, 33–36). This similarity in the reaction

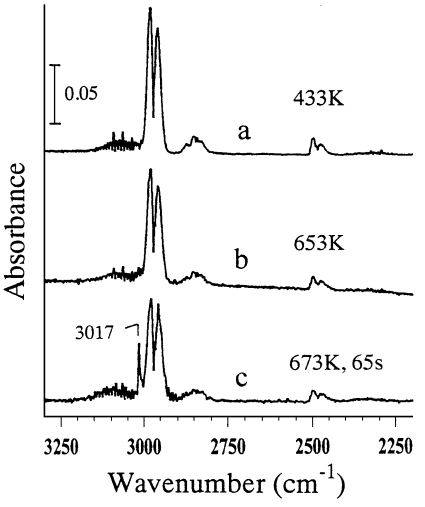

FIG. 3. Variation of the IR spectrum of the TiO_2, initially in contact with ~20 Torr of CH_3I at 308 K, with temperature. (a and b) Spectra taken at 433 and 653 K, respectively, while the TiO_2 sample was linearly heated to 673 K at 2 K/s. (c) Spectrum taken after the TiO_2 temperature was held at 673 K for 65 s. All of the spectra were recorded with five scans. The TiO_2 sample used was ~30 mg.

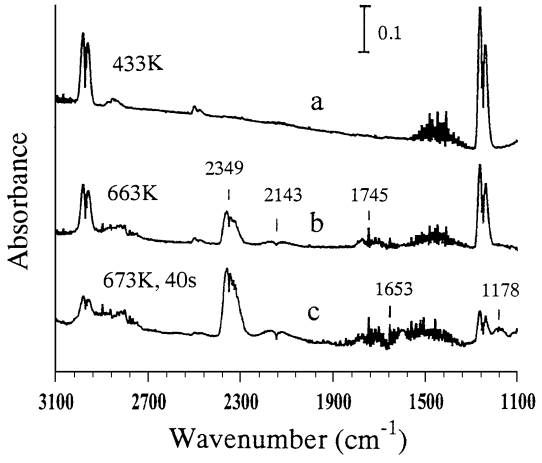

FIG. 4. Variation of the IR spectrum of the TiO_2, initially in contact with a mixture of ~25 Torr of CH_3I and ~70 Torr of O_2 at 308 K, with temperature. (a and b) Spectra taken at 433 and 663 K, respectively, while the TiO_2 sample was linearly heated to 673 K at 2 K/s. (c) Spectrum taken after the TiO_2 temperature was held at 673 K for 40 s. All of the spectra were recorded with five scans. The TiO_2 sample used was ~30 mg.

pathways and reaction kinetics suggests the same reaction-initiating surface intermediate, i.e., $CH_3O_{(a)}$, is formed in the present study of CH_3I interacting with TiO_2. This argument is consistent with the result shown in Fig. 2, which indicates the formation of methoxy species due to CH_3I decomposition. Figure 5b shows the continuing changes of the gaseous compounds as a function of time as the TiO_2 sample is held at 673 K. While CH_3I declines continuously, $CH_2O_{(g)}$, and $(CH_3)_2O_{(g)}$ keep increasing, reaching their maxima at ~30 and ~80 s, respectively and then decrease slowly. $CO_{(g)}$ also shows a maximum at ~300 s and decreases slightly upon further annealing, presumably due to oxidation to monotonically increased $CO_{2(g)}$. $H_2O_{(g)}$ reaches its maximum at ~80 s and gradually decreases up to ~380 s, and then becomes almost constant. This decrease in the period of 80–380 s proceeds concurrently with the increase of surface hydroxyl groups as observed by IR spectroscopy in the range of 3600–3800 cm^{-1} (not shown).

Photooxidation of CH_3I on Powdered TiO_2

The photochemistry of CH_3I over powdered TiO_2 was studied in the absence and in the presence of O_2. Figure 6a shows the spectrum for the TiO_2 at 308 K in contact with a mixture of 2 Torr of CH_3I and 10 Torr of O_2. After 3 h of photoillumination, $CO_{2(g)}$ and surface formate groups ($HCOO_{(a)}$, 1360, 1381, 1551, and 2870 cm^{-1}) (25, 37) are observed as shown in Fig. 6b. From the differential spectrum shown in Fig. 6c, the surface amount of adsorbed CH_3I (1245 and 2955 cm^{-1}) is considerably decreased. This decrease may be due to a combination effect of formate site blocking, surface heating upon the UV irradiation, and consumption by photoreaction. Because the TiO_2 surface temperature was raised to ~330 K upon UV irradiation, a thermal control experiment was carried out as well. In this experiment, the TiO_2 was exposed to a mixture of 2 Torr of CH_3I and 10 Torr of O_2 and the IR spectrum was then monitored as a function of time while the TiO_2 sample was held at this temperature. It was found that the formation of formate groups was negligible after 3 h of annealing at 330 K. Furthermore, since methoxy groups are generated after CH_3I dissociative adsorption on the TiO_2 surface, the role of methoxy groups in the photooxidation was also investigated. A methoxy-covered TiO_2 surface was prepared by exposing a clean TiO_2 to 2 Torr of methanol followed by evacuation at 523 K for 1 min (23–25). Figure 6d shows the spectrum of this methoxy-covered TiO_2 sample at 308 K in contact with 10 Torr of O_2. Figure 6e shows the results

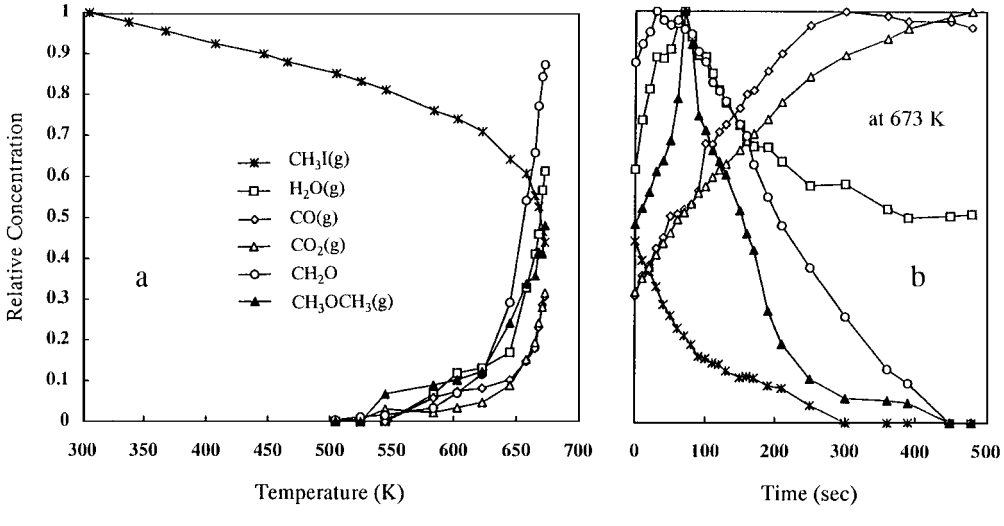

FIG. 5. Relative concentrations of the gaseous intermediates and products as a function of TiO_2 temperature (a) and as a function of time at 673 K (b). The maximum amount detected in the heating process for each intermediate and product is scaled to 1.

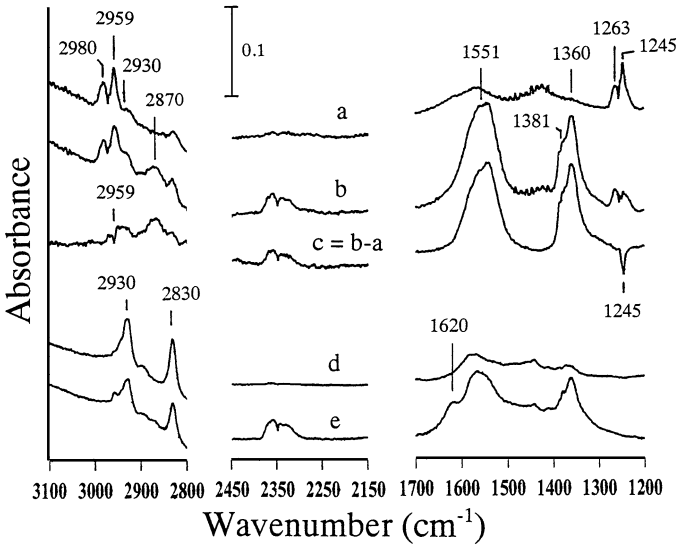

FIG. 6. IR spectra of TiO_2 in contact with a mixture of 2 Torr CH_3I and 10 Torr O_2 before irradiation (a) and after 180 min of irradiation (b). The TiO_2 sample used was ~35 mg. (c) Net spectrum obtained by subtracting (b) from (a). (d and e) Spectra of methoxy-covered TiO_2 before irradiation and after 150 min of irradiation in 10 Torr of O_2, respectively. The TiO_2 sample used was ~30 mg. The methoxy-covered TiO_2 surface was prepared by exposing clean TiO_2 to 2 Torr of methanol followed by evacuation at 523 K for 1 min. All the traces in the range of 2800–3100 cm^{-1} are multiplied by 2 and those in the range of 2050–2450 cm^{-1} are multiplied by 3. All of the spectra were taken with five scans.

of the photochemistry of the surface methoxy groups in the presence of O_2. It is found that in addition to formate formation, surface water ($H_2O_{(a)}$, 1620 cm^{-1}) is concomitantly formed during the irradiation. A similar observation has been reported for methoxy groups irradiated at 320 nm in the presence of O_2 (24). The major difference between the photochemistry of methoxy groups and CH_3I is the relative concentration of surface water to formate formed. This value is much higher for methoxy groups, indicating that the major contribution for the formate formation in the photooxidation of CH_3I over TiO_2 is not from adsorbed methoxy groups. The possible intermediate to initiate the surface photochemistry of CH_3I on TiO_2 will be discussed in the next section. On the other hand, in the study of photoillumination of the TiO_2 sample in 2 Torr of CH_3I in the absence of O_2, although the high-frequency end of the light source used in this experiment may decompose CH_3I, however, probably due to slow reaction rate, no gaseous or surface species other than CH_3I and surface methoxy groups are detected after 2 h of illumination.

Temperature-Programmed Desorption Study of CH_3I on TiO_2(110)

The adsorption and photochemistry of methyl iodide on TiO_2(110) have been reported recently by Garrett *et al.* (12, 13). In their TPD study, methyl iodide is desorbed with complex behavior due to the presence of surface defects and repulsive lateral interactions between the adsorbed molecules. At low coverages, methyl iodide is adsorbed more strongly at the defect sites and is desorbed at ~210 K. Increasing the coverage, the methyl iodide desorption peak shifts to lower temperatures, reaching ~150 K at one monolayer. The multilayer CH_3I is desorbed with peaks at 130–145 K. Similar methyl iodide molecular desorption is observed in the present study and therefore no TPD results are intended to be presented here. In our study, a exposure of ~2.4 l corresponds to 1 ML. In addition to the molecular desorption, an extensive mass search was performed for higher CH_3I coverages in the TPD study to identify other possible desorption products. Figure 7 shows the TiO_2(110) TPD spectra of dimethyl ether represented by the $m/e = 45$ ion at the indicated exposures for a smoothed surface and a sputtered surface (prepared by Ar^+ bombardment at 500 eV, 2 μA, and 300 K). The dimethyl ether evolution is identified by comparing the fragmentation pattern obtained from the integrated TPD peak area at the masses of 29, 30, 45, and 46 amu to the standard mass spectrum (38). Dimethyl ether shows a single desorption peak, for all of the exposures in Fig. 7, with lower peak temperatures at higher CH_3I exposures. Note that formation of dimethyl ether occurs only at multilayer coverages. Since the methyl

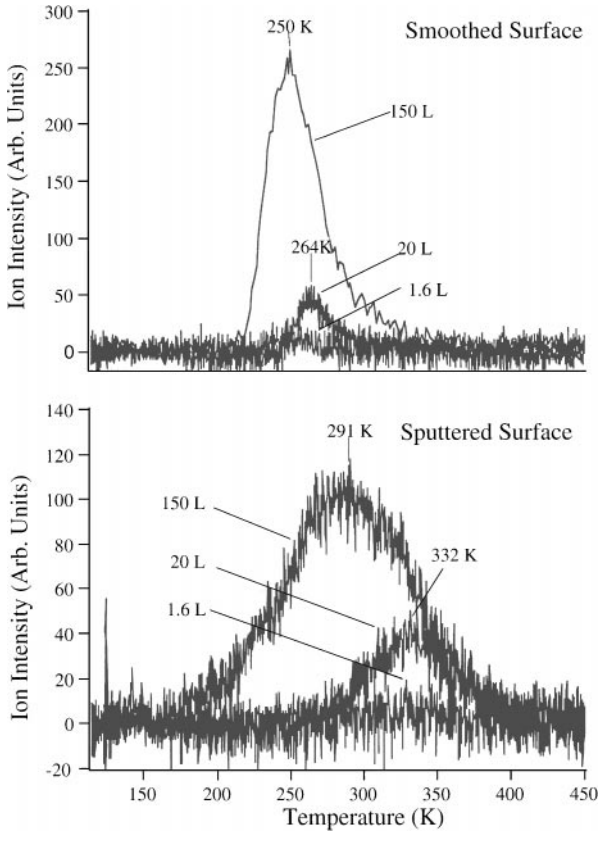

FIG. 7. Temperature-programmed desorption spectra of dimethyl ether represented by the $m/e = 45$ ion at the indicated CH_3I exposures for a smoothed (upper panel) and a sputtered (lower panel) TiO_2(110) surface.

iodide is completely desorbed from the surface by 250 K, the evolution of dimethyl ether is very likely limited by its desorption step. Compared to the case of the smoothed surface, the TPD peaks from the sputtered surface are much broader and shifted to higher temperatures, reflecting the effect of surface site heterogeneity and higher desorption energy for dimethyl ether from the sputtered TiO_2(110) surface. No iodine-containing products were detected within our QMS detection limit in TPD experiments.

XPS has been used complementarily to monitor the surface species for the TiO_2 surface which was previously exposed to 150 l of methyl iodide at 115 K followed by linear heating to 350 K. No carbon- or iodine-containing species on the surface are detected after the heating other than titanium and oxygen. This result indicates that either all the C and I have been desorbed from the surface by 350 K or the amount of CH_3I reacting with the surface is so small that the surface species resulting from CH_3I decomposition cannot be detected by our X-ray photoemission spectrometer. The previous study by Garrett *et al.* has shown that the I($3d_{5/2}$) core level photoemission peak for molecularly adsorbed methyl iodide on TiO_2(110) is at 620.2 eV, while that of the adsorbed iodine produced by UV irradiation of the adsorbed methyl iodide is at 618.7 eV (12, 13). Since the thermal reactions as shown in the present study are induced by C–I bond dissociation of adsorbed methyl iodide, iodine atoms would have to be left on the surface. Therefore, its stability with respect to temperature was further studied by XPS for the sputtered TiO_2(110) surface. It has been reported that X-ray irradiation is able to induce chemical change in the methyl iodide layer adsorbed on TiO_2(110) (13). Accordingly, a similar procedure was followed in the present study to dissociate the adsorbed methyl iodide layer to generate surface iodine. Figure 8 shows the change of the I($3d_{5/2}$) photoemission peak for the sputtered TiO_2 surface previously exposed to 8 l of methyl iodide at 105 K followed by X-ray irradiation for 20 min and flashing to the indicated temperatures. For the trace at 115 K, the peak is located at 621.4 eV which is attributed to the remaining adsorbed methyl iodide ($CH_3I_{(a)}$) after X-ray irradiation and a small surface temperature increase. After temperature was flashed to 253 K to desorb the remaining $CH_3I_{(a)}$, a peak at 619.8 eV, albeit small, is clearly observed. Compared to the previous assignment for the surface iodine photoemission, this peak is attributed to the adsorbed iodine ($I_{(a)}$) (12, 13). It can be completely desorbed from the surface by 570 K. The slight differences in the binding energies for $CH_3I_{(a)}$ and $I_{(a)}$ observed here and those in Garrett's work could be due to the spectrometer work function calibration.

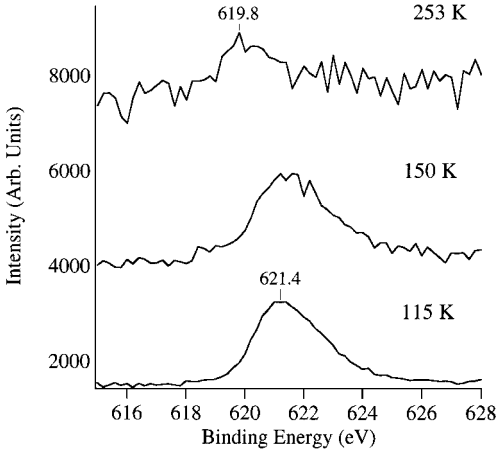

FIG. 8. XPS I($3d_{5/2}$) spectra of the sputtered TiO_2 surface previously exposed to 8 L of methyl iodide at 105 K followed by X-ray irradiation for 20 min and flashing to the indicated temperatures.

DISCUSSION

From the IR study, CH_3I is adsorbed on powdered TiO_2 in two different forms. One is reversibly adsorbed molecular CH_3I. The other one is methoxy groups from CH_3I decomposition. In the absence of oxygen, the methoxy groups further dissociate to generate methane as a major thermal product. In the presence of oxygen, $CH_2O_{(g)}$, $(CH_3)_2O_{(g)}$, $CO_{(g)}$, $CO_{2(g)}$, and $H_2O_{(g)}$ are produced and the channel for the formation of methane is terminated. In the previous study of alcohol reactions on TiO_2, Barteau *et al.* have proposed different reaction pathways for the gaseous reaction products (34, 35, 39). It is suggested that CH_4 formation from methoxy decomposition is initiated by C–O bond scission to fill surface oxygen vacancies, forming CH_3 species. A portion of these methyl groups may dissociate to generate surface hydrogen which instantaneously reacts with the remaining methyl groups to form methane. Presumably, when oxygen is present in the gas phase and the surface oxygen vacancies are effectively filled with dissociatively adsorbed O_2, the methane production channel is terminated. In this case, surface methoxy groups would follow another pathway to form oxygen-containing compounds. It may dehydrogenate to form formaldehyde which reacts with TiO_2 surfaces to produce adsorbed formate (37). Decomposition of the formate groups results in the formation/desorption of carbon monoxide and carbon dioxide from the surfaces (34–36). Dimethyl ether is the reaction product from coupling of two adsorbed methoxy groups (34, 39). In the present study, formation of dimethyl ether was also found in the TPD study of CH_3I adsorbed on a single-crystal TiO_2(110) surface, but it occurs only at multilayer coverages. If the mechanism for the formation of dimethyl ether on TiO_2(110) is same as that on powdered TiO_2, dimethyl ether is expected to be observed at monolayer coverage. However, this is not the case, implying another reaction mechanism must exist. Furthermore, the formation temperature of $(CH_3)_2O$ on TiO_2(110) is much lower than that on powdered TiO_2. Two possibilities, for the $(CH_3)_2O$ yield that appears to scale

with multilayer exposure, due to CH_3I contamination with $(CH_3)_2O$ or electron-induced reaction during TPD study have been ruled out. It was found that no cracking pattern for $(CH_3)_2O$ was observed by our mass spectrometer at 10^{-6} Torr of CH_3I backing pressure and that similar results were obtained in the TPD study of CH_3I on TiO_2 with a negative sample bias at -65 V to repel possible strayed electrons emitting from our mass spectrometer operated at -55 V bias at electron source (filaments). There is a well-known reaction in the condensed phase called "Williamson synthesis" in which alkoxide ions attack alkyl halides to form ether (40). Therefore, it is postulated that on single-crystal TiO_2(110), methoxide ions may be produced by simultaneously breaking CH_3–I and Ti–O bonds and forming a CH_3–O bond and then migrating into the CH_3I multilayer where they nucleophilically attack CH_3I, generating dimethyl ether which subsequently diffuses back to adsorb directly at the TiO_2 surface. The following desorption of dimethyl ether from TiO_2 is the rate-limiting step for its evolution in the TPD study and depends on the surface heterogeneity as observed in Fig. 7. In the present study, the presence of a multilayer may induce the surface reaction by promoting the dissociation of adsorbate molecules in the monolayer. Recently, in the study of activation of cyclobutane on Ru(001), Hagedorn *et al.* have reported multilayer-assisted decomposition of the adsorbates in the monolayer at a temperature at which the monolayer would not dissociate without the multilayer (41). The electron-induced chemical reaction on alkyl halide films, though it has been reported by White *et al.* (42), is unlikely in our experiment. The formation of dimethyl ether was also observed with sample negatively biased to the mass spectrometer to prevent electrons from reaching the surface.

Since all of the reactions on TiO_2 surfaces are initiated by decomposition of CH_3I, more specifically speaking, by C–I bond dissociation to produce methoxy species, we discuss here the mechanism for CH_3I decomposition in this study by comparing the previously proposed mechanisms for the formation of methoxy groups from other precursor molecules, such as CH_3OH and CH_3Cl, on various oxidic surfaces. In the case of methanol decomposition forming methoxy groups on TiO_2, in previous studies two origins have been proposed (34, 36, 39). Methanol may react with surface hydroxyl groups to form methoxy and water. This reaction pathway has been shown to be suppressed as TiO_2 sample is pretreated at 673 K to largely remove surface hydroxyl groups. In the previous study of CH_3Cl dissociation on a thin layer of alumina, Beebe *et al.* have found that surface hydroxyl groups are consumed, accompanied with the formation of surface methoxy groups (43). These data implicate the involvement of surface hydroxyl groups in the C–Cl bond dissociation as well as in the methoxy formation. The other channel for the formation of methoxy species may occur at coordinatively unsaturated TiO_2 cations through dehydrogenation of methanol by neighboring surface oxygens. Dissociative adsorption of methanol without involvement of surface hydroxyl groups has also been observed on mangesium oxide (44), germanium oxide (45), silicon oxide (46, 47), and aluminum oxide (48). As to the mechanism for the CH_3I decomposition in the present work, the formation of dimethyl ether due to CH_3I reaction on the hydroxyl-free TiO_2(110) single-crystal surface seems to suggest that hydroxyl groups are unnecessary for the C–I bond scission. Assuming that the adsorbed CH_3I is bonded to the Ti ions via iodine atom, the scission of the C–I bond probably proceeds by nucleophilic attack at the methyl carbon from TiO_2 surface oxygen anions. However, the surface hydroxyl groups play an important role in the C–I bond breakage for the enhanced formation of methoxy groups as shown in Fig. 2. This enhancement occurs at the expense of hydroxyl groups only at 3675 and 3724 cm^{-1}. It is interesting to find that only certain types of OH groups assist the CH_3I decomposition, probably via nucleophilic attack of basic hydroxyl groups. Primet *et al.* have shown the basic character for the hydroxyl groups on anatase and rutile TiO_2 by using CO_2 as probing molecules (49). In addition, Che *et al.* have detected $TCNE^-$ and TNB^- radical ions during the adsorption of tetracyanoethylene and trinitrobenzene on anatase TiO_2 which are attributed to the presence of OH^- groups on the surface (50). The difference in thermal reactivity for CH_3I on powdered TiO_2 and on single-crystal TiO_2 surfaces can be attributed to the presence of various crystallographic facets, defects, and hydroxyl groups on the former surface.

For photochemistry of CH_3I over powdered TiO_2, no spectroscopic evidence shows that CH_3I photoreaction takes place in the absence of O_2. In contrast, as O_2 is present, formate and $CO_{2(g)}$ are formed as major products. Previous studies have shown that $CO_{2(g)}$ is derived from photooxidation of formate groups (51, 52). Wong *et al.* have studied the photooxidation of CH_3Cl on powdered TiO_2 in the presence of O_2 using the full wavelength emitted from a 350-W Hg arc lamp (11). They have proposed a radical-mediated mechanism, initiated by superoxide, O_2^-, from the combination of photoelectrons and absorbed oxygen on the TiO_2 surface, to explain the formation of CH_2Cl_2. It is believed that the photoreactions in the present study may also be initiated by superoxide, O_2^-. Because it has been reported that on TiO_2 surfaces upon UV irradiation at 77 K, EPR (electron paramagnetic resonance) shows the existence of O_3^-, O_3^{3-}, and O_2^- species and only the last one is shown to be stable at room temperature (53). In the present study of CH_3I photochemistry on powdered TiO_2 in O_2 to form formate, since no kinetically short-lived intermediates are detected, no detailed reaction pathways are presented here. However, the related results from previous studies may provide insights into the formate formation. Jenkin

et al. have found the formation of CH_2O and HCOOH during the reaction of CH_3O radicals and O_2 in the gas phase (54). If CH_3O radicals are formed near the TiO_2 surface in the present photochemistry study of CH_3I in O_2, the reaction products of CH_2O and HCOOH from the reaction of CH_3O radicals and O_2 may react with the TiO_2 surface to form formate groups (25, 37). CH_3O radicals are one of the thermolytic or photolytic products of CH_3OOCH_3 (55–57) which have been observed in the interaction of methyl halides with superoxide ions (O_2^-) in aprotic solvents (58). Another origin for the formation of CH_3O radicals is the decomposition of CH_3O_2 (59) which may result from the interaction of CH_3I with O_2^- on the TiO_2 surface.

CONCLUSIONS

Our experiments on the interaction of CH_3I with TiO_2 were carried out on powdered and single-crystal surfaces. On the powdered surface, it belongs to the solid–gas interaction for the experimental conditions used. CH_3I dissociates on this surface to form $CH_3O_{(a)}$. Its dissociation rate is enhanced by the presence of isolated hydroxyl groups. In the thermal chemistry, $CH_{4(g)}$ is the major product in the absence of O_2. However, only oxygen-containing intermediates and products of $CH_2O_{(g)}$, $(CH_3)_2O_{(g)}$, $CO_{(g)}$, $CO_{2(g)}$, and $H_2O_{(g)}$ are produced in the presence of O_2. In the photochemistry, O_2 is crucial for CH_3I oxidation. On the TiO_2 single crystal, the TPD experiment was performed with a multilayer of CH_3I. It makes a link to the solid–liquid interaction (41). In the TPD study, $(CH_3)_2O$ is also found to be the desorption product. $(CH_3)_2O$ is formed on both surfaces; however, its appearance temperatures are very different, indicating different operative mechanisms. On the powdered surface, it comes from coupling of two $CH_3O_{(a)}$. On the other hand, it may be due to "Williamson synthesis" on the single crystal at multilayer coverages.

ACKNOWLEDGMENTS

We gratefully acknowledge the financial support of the National Science Council of the Republic of China (Grants NSC-88-2113-M-006-014 and NSC-88-2113-M-001-025) for this research.

REFERENCES

1. Bent, B. E., *Chem. Rev.* **96**, 1361 (1996).
2. Bol, C. W. J., and Friend, C. M., *J. Phys. Chem.* **99**, 11930 (1995).
3. Solymosi, F., and Klivenyi, G., *J. Phys. Chem.* **99**, 8950 (1995).
4. Zhou, X.-L., Liu, Z.-M., Kiss, J., Sloan, D. W., and White, J. M., *J. Am. Chem. Soc.* **117**, 3565 (1995).
5. Solymosi, F., and Rasko, J., *J. Catal.* **155**, 74 (1995).
6. Rasko, J., Bontovics, J., and Solymosi, F., *J. Catal.* **143**, 138 (1993).
7. McGee, K. C., Driessen, M. D., and Grassian, V. H., *J. Catal.* **157**, 730 (1995).
8. Driessen, M. D., and Grassian, V. H., *J. Am. Chem. Soc.* **119**, 1697 (1997).
9. Hoffmann, M. R., Martin, S. T., Choi, W., and Bahnemann, D. W., *Chem. Rev.* **95**, 69 (1995).
10. Fox, M. A., and Dulay, M. T., *Chem. Rev.* **93**, 341 (1993).
11. Wong, J. C. S., Linsebigler, A., Lu, G., Fan, J., and Yates, Jr., J. T., *J. Phys. Chem.* **99**, 335 (1995).
12. Garrett, S. J., Holbert, V. P., Stair, P. C., and Weitz, E., *J. Chem. Phys.* **100**, 4626 (1994).
13. Garrett, S. J., Holbert, V. P., Stair, P. C., and Weitz, E., *J. Chem. Phys.* **100**, 4615 (1994).
14. Basu, P., Ballinger, T. H., and Yates, Jr., J. T., *Rev. Sci. Instrum.* **59**, 1321 (1988).
15. Fan, J., and Yates, Jr., J. T., *J. Phys. Chem.* **98**, 10621 (1994).
16. Su, C., Song, K.-J., Wang, Y. L., Lu, H.-L., Chuang, T. J., and Lin, J.-C., *J. Chem. Phys.* **107**, 7543 (1997).
17. Lin, J.-C., Chen, K.-H., Chang, H.-C., Tsai, C.-S., Lin, C.-E., and Wang, J.-K., *J. Chem. Phys.* **105**, 3975 (1996).
18. Linsebigler, A., Lu, G., and Yates, Jr., J. T., *Chem. Rev.* **95**, 735 (1995).
19. Pan, J.-M., Maschhoff, B. L., Diebold, U., and Madey, T. E., *J. Vac. Sci. Technol. A* **10**, 2470 (1992).
20. Shimanouchi, T., "Tables of Molecular Vibrational Frequencies," Vol. 1. NSRDS, National Bureau of Standards, Washington, DC, 1972.
21. "CRC Hand Book of Chemistry and Physics" (D. R. Lide, Ed.), 71st edition, 1990–1991, pp. 6–54. CRC Press, Boca Raton, FL, 1991.
22. Souda, R., Hayami, W., Aizawa, T., and Ishizawa, Y., *Surf. Sci.* **285**, 265 (1993).
23. Taylor, E. A., and Griffin, G. L., *J. Phys. Chem.* **92**, 477 (1988).
24. Chuang, C.-C., Chen, C.-C., and Lin, J.-L., *J. Phys. Chem. B* **103**, 2439 (1999).
25. Chuang, C.-C., Wu, W.-C., Huang, M.-C., Huang, I.-C., and Lin, J.-L., *J. Catal.* **185**, 423 (1999).
26. Tanaka, K., and White, J. M., *J. Phys. Chem.* **86**, 4708 (1982).
27. Primet, M. , Pichat, P., and Mathieu, M. V., *J. Phys. Chem.* **75**, 1216 (1971).
28. Yates, D. J. C., *J. Phys. Chem.* **65**, 746 (1961).
29. Jackson, P., and Parfitt, G. D., *Trans. Faraday Soc.* **67**, 2469 (1971).
30. Jones, P., and Hockey, J. A., *Trans. Faraday Soc.* **67**, 2469 (1971).
31. Lewis, K. E., and Parffit, G. D., *Trans. Faraday Soc.* **62**, 204 (1966).
32. "The Aldrich Library of FT-IR Spectra," 1st edition. Aldrich, Milwaukee, WI, 1985.
33. Suda, Y., Morimoto, T., and Nagao, M., *Langmuir* **3**, 99 (1987).
34. Lusvardi, V. S., Barteau, M. A., and Farneth, W. E., *J. Catal.* **153**, 41 (1995).
35. Kim, K. S., Barteau, M. A., and Farneth, W. E., *Langmuir* **4**, 533 (1988).
36. Hussein, G. A. M., Sheppard, N., Zaki, M. I., and Fahim, R. B., *J. Chem. Soc., Faraday Trans.* **87**, 2655 (1991).
37. Busca, G., Lamotte, J., Lavalley, J.-C., and Lorenzelli, V., *J. Am. Chem. Soc.* **109**, 5197 (1987).
38. "Eight Peak Index of Mass Spectra," 4th edition. The Royal Chem. Soc., London 1991 (ISBN-085186-417-1).
39. Kim, K. S., and Barteau, M. A., *Surf. Sci.* **223**, 13 (1989).
40. Morrison, R. T., and Boyd, R. N., "Organic Chemistry," 3rd edition. Allyn and Bacon, Inc., Boston, 1973.
41. Hagedorn, C. J., Weiss, M. J., and Weinberg, W. H., *J. Am. Chem. Soc.* **120**, 11825 (1998).
42. Zhou, X.-L., Blass, P. M., Koel, B. E., White, J. M., *Surf. Sci.* **271**, 452 (1992).
43. Beebe, T. P. J., Crowell, J. E., and Yates, Jr., J. T., *J. Phys. Chem.* **92**, 1296 (1988).
44. Tench, A. J., Giles, D., and Kibblewhite, J. F., *Trans. Faraday Soc.* **67**, 854 (1967).
45. Mcmanus, J. C., Matsushita, K.-I., and Low, M. J., *Can. J. Chem.* **47**, 1077 (1969).

46. Borello, E., Zecchina, A., and Morterra, C., *J. Phys. Chem.* **71**, 2945 (1967).
47. Borello, E., Zecchina, A., and Morterra, C., *J. Phys. Chem.* **71**, 2938 (1967).
48. Kagel, R. O., *J. Phys. Chem.* **71**, 844 (1967).
49. Primet, M., Pichat, P., and Mathieu, M. V., *J. Phys. Chem.* **75**, 1221 (1971).
50. Che, M., Naccache, C., and Imelik, B., *J. Catal.* **24**, 328 (1972).
51. Carraway, E. R., Hoffman, A. J., and Hoffmann, M. R., *Environ. Sci. Technol.* **28**, 786 (1994).
52. Morison, S. R., and Freund, T., *J. Chem. Phys.* **47**, 1543 (1967).
53. Meriaudeau, P., and Vedrine, J. C., *J. Chem. Soc., Faraday Trans. 2* **72**, 472 (1976).
54. Jenkin, M. E., Hayman, G. D., and Cox, R. A., *J. Photochem. Photobiol. A: Chem.* **42**, 187 (1988).
55. Takezaki, Y., Miyazaki, T., and Nakahara, N., *J. Chem. Phys.* **25**, 536 (1956).
56. Takezaki, Y., and Takeuchi, C., *J. Chem. Phys.* **22**, 1527 (1954).
57. Toth, L. M., and Johnston, H. S., *J. Am. Chem. Soc.* **91**, 1276 (1969).
58. Roberts, J. L. J., and Sawyer, D. T., *J. Am. Chem. Soc.* **103**, 712 (1981).
59. Cobos, C. J., Hippler, H., Luther, K., Ravishankara, A. R., and Troe, J., *J. Phys. Chem.* **89**, 4332 (1985).